International Journal of Pure and Applied Physics.
ISSN 0973-1776 Volume 8, Number 2 (2012), pp. 99-111

http://www.ripublication.com/ijpap.htm

GPR Survey at the Archaeological Roman Site of Turaniana, Almeria, Spain

[1]A. Faize, [1]A. Driouach and [1]M. Essaaidi,
[2]C. Moreno de Jong van Coevorden, [2]C. Cobos Sanchez,
[2]M. Fernandez Pantoja, [2]S. Gonzalez Garcia, [2]A. Rubio Bretones
and [2]Rafael Gomez

[1]Electomagnetism Group Electromagnetism and Physics Matter Department,
University of Tetouan, Morocco
[2]Martin Group Electromagnetism and Physics Matter Department,
University of Granada, Spain
E-mail: ahmedfaize6@hotmail.com

Abstract

The exploration of sites of potential archaeological interest is a time consuming and strenuous exercise. The advent of economically feasible geophysical sensing methods has significantly altered the landscape for identifying and evaluating potential sites and detecting variances on the surface. This paper evaluates the use of Ground Penetrating Radar to acquire and process data on an archeological site in Turaniana in Southern Spain. Results from four areas within a target zone were evaluated with the help of 3D Visualization. Several structures within these areas were identified to be of promising nature and would be ideal locations for excavation for an in-depth analysis.

Index Terms: GPR, Turaniana Site, Archeology, FDTD

Introduction

Ground Penetrating Radar (GPR) is geophysical sensing system that utilizes electromagnetic energy to determine surface variances. This system provides a non-destructive method, which is used extensively in a variety of applications and in several fields, including mine detection [1], revelation of cracks in marble quarries

[2], road-rail way evaluations [3], or like in the present work for sites with archaeological interest survey [4], [5]. GPR is the most feasible and friendly instrumentation to detect buried remains and to perform diagnostics of archaeological structures with the aim of detecting hidden objects. For other side, GPR technique allows performing measurements over large areas in very fast way.

Excavation is often more expensive, but the GPR technique offers a logical answer to this dilemma by delivering increasingly accurate data regarding site stratigraphy, the location and depths of covered anomalies. GPR equipment is not expensive; however the cost of this technology has decreased in recent years, prompting more and more archaeologists to take advantage of this growing technology. In this paper, the equipment employed for the survey was a Mala ProEx GPR system with a 500 MHz and 800 MHz antenna.

Such methodologies along with powerful 3D visualization techniques are widely applied in GPR surveys with archaeological purpose [6, 9]. These surveys are usually image sites containing continuous linear features extending over several meters length such as foundation, walls, ditches, etc.

The present work describes the GPR investigation performed at the archaeological site of Roquetas de Mar, Turaniana region of Almeria (Spain). The particular goal of the GPR survey is to locate the most promising areas within the archaeological site to help the archaeologists in their explorations tasks.

The rest of the present work is organized as follows: in section 3 which describes the archaeological site; section 4 explains GPR data acquisition and processing techniques; section 5 presents the results and discussion, and finally the conclusions of this work researches are given in section 6.

Site Description

Situated on the southwest of Almeria, Roquetas de Mar used to be a traditional fishing village. Founded by the Phoenicians and Greeks, it was named Turaniana during the Roman times. This town, a true gem of the area, combines the facilities of a city with the relaxation of beach life.

The earliest remains found in the area is dated from the Neolithic and the culture of Los Millares. There are also remains from the Bronze Age, though the area enjoyed its first splendor since the arrival of the Phoenicians.

The area is characterized by many Roman remain from the times when Adra became an important Mediterranean town thanks due to the trade of salted fish and the precious “garum”, a fermented fish sauce that the Romans loved. Vergi (Berja), Turaniana (Roquetas de Mar) and Murgi, in the municipality of El Ejido, are other examples of Roman towns.

In this paper, we selected four areas from nine, using GPR system. These four areas present valuable archaeological information.

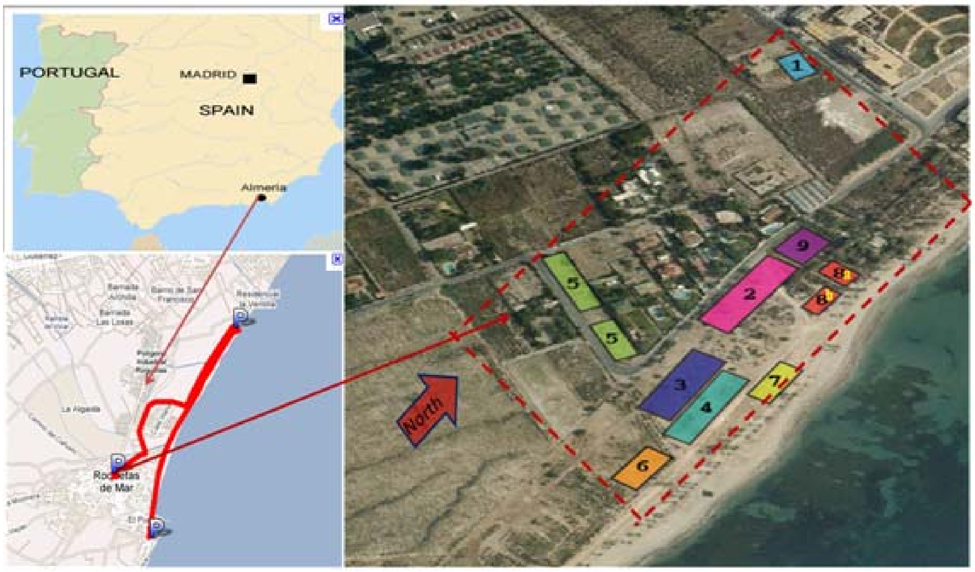

Figure 1: Location map of the Turaniana Almeria Spain (Europe)

GPR Data Acquisition and Processing

GPR data were processed primarily using Reflexw software [10]. The equipment employed the survey was Mala ProEx GPR system with 500 MHz and 800 MHz antennas simultaneously using the rough terrain cart. This configuration is optimal to detect shallow and deeper anomalies with detail, being half less time consuming than surveying each area separately with each antenna. At each site radar profiles were collected parallel across the survey grids. The horizontal spacing between parallel profiles at the site was 0.40 m. Radar reflections along the survey lines were recorded continuously across the ground each 2cm, with a stack = 2; along each profiles. All radar reflections within 46ns (500MHz antenna) and 30ns (800MHz antenna) (two-way travel time) time window were recorded digitally in the field as 16 bit data and 700 samples per radar scan.

Four Areas were selected (area 4, 7, 8 and 9) among nine to carry out the archaeological detail prospection GPR survey (Fig 1). The following table 1 describes all detail as far as concerned these areas.

Table 1: Description of the four areas selected in this study

Area	Dimensions (M)	Number of Lines
Area 4	10 x 30	26
Area 7	16 x 10	41
Area 8	15 x 15	38
Area 9	16 x 10	41

The areas of data processing have been grouped under the headings: data editing, basic processing, interpretation processing, and visualization processing.

Processing in this location is usually done when a good head of information about a site is available and need for the processing has been defined which achieves a final objective. Each B-Scan was filtered using Reflexw V 4.5 software by applying the processing sequences described in Table 2.

Table 2: Sequence Processing Applied To The Gpr Data Acquired With The 500 And 800 Mhz Shielded Antennas

GPR PROCESSING SEQUENCE SCAN 3D (REFELXW V4.2) / GPR-SLICE V7	
z	800 MHz
Dewow filtering (2.4 ns)	Dewow filtering (1.25 ns)
Bandpass Frequency (Lower Cuttof =120; Lower Plateau=180; Upper Plateau=800 ; Upper Cuttof=920)	Bandpass Frequency (Lower Cuttof =280; Lower Plateau=460; Upper Plateau=1600 ; Upper Cuttof=1800)
Energy decay (Scaling Value= 0.10)	Energy decay (Scaling Value= 0.10)
Running average (Average traces=6; Start time=0; End Time=46)	Running average (Average traces=6; Start time= 0; End time= 36.77)
Background removal based on all traces	Background removal based on all traces
Export to GPR-SLICE	Export to GPR-SLICE
Generation of two 3D data cubes following pseudo 3D and full-resolution processing schemes	Generation of two 3D data cubes following pseudo 3D and full-resolution processing schemes

Results and Discussion

With the knowledge of what to look for, data interpretation, while not easy, will in time become much less confusing.

Some buried targets create unique GPR reflections. An understanding of why each type of signature appears as it does, will allow the researcher to interpret many common subsurface anomalies in the field.

From all the data acquired, for sake of brevity only the 4, 7, 8 and 9 for explored areas are showed. The next subsections show the results of the GPR survey in these areas.

Area 4

Two profiles taken using the 500 MHz and 800 MHz antennas (Fig 2) allow location of structures such as buildings, walls… etc. The radargrams were filtered using the processing described in table 2.

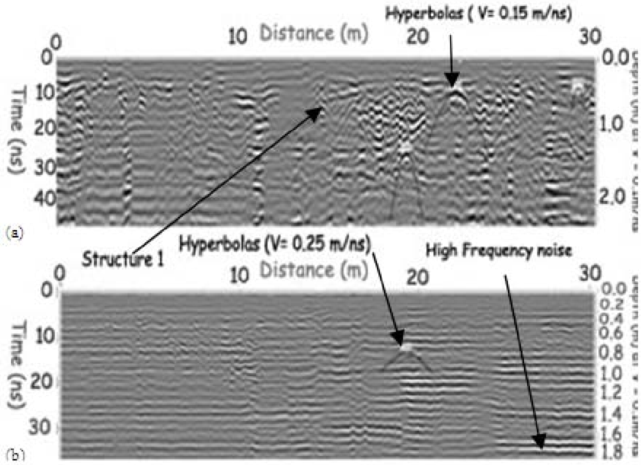

Figure 2: Processed Radargrams (Area 4) (B-Scan) achievement with 500 MHz antenna from line 5 (A) and with 800 MHz antenna from line 20 (B)

The structure 1 is visible at 0.5 meters depth between 14 m- 20 m, and an en evident hyperbola (0.15 m/ns) obtained by 500 MHz antenna, quite significant, but associated with a bump (fig 2a) and is thought to be the Romans remains. Also, Fig 2b shows structure 1 located between 8 m- 12 m at 0.8 m depth and an evident hyperbola (0.25 m/ns) obtained by 800 MHz antenna.

We assume that this strongly different value of propagation velocity is caused by the different electromagnetic properties of the soil where the mound was located, i.e. greater humidity.

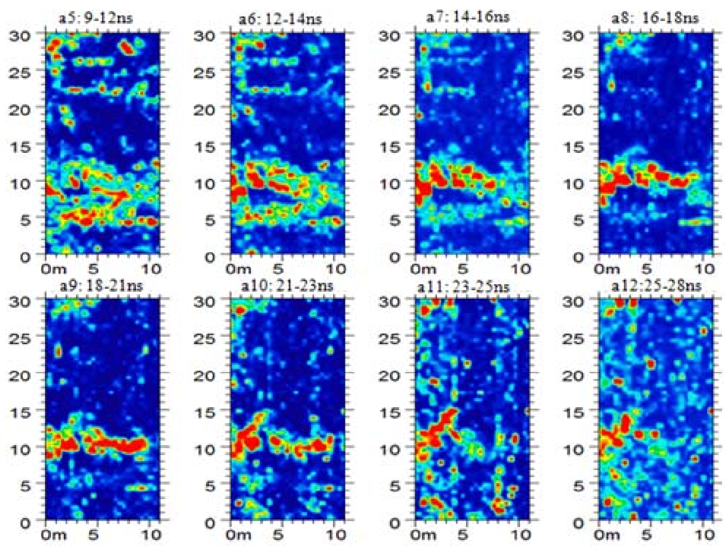

Figure 3: Time-Slice (C-Scan) of area 4 at 9ns-28 ns with 500 MHz antenna

Figure 3 illustrate a horizontal slice between 9- 28 ns. This time slice was built with the data collected with the 500 MHz antenna. The strongest radar reflection is seen crossing this area. This signal was created by a modern utility ditch and it obscures a large portion of potential features in its vicinity. Other deeper radar reflections indicate the main anomaly that exist well below 1 meter (8 -25 ns) (structure 1). Determining the age, function, and historical significance of this anomaly will require archaeological excavation for ground truthing. These features also might be better understood by a more complete GPR survey coverage of this area of the fort grounds.

Grouping more scans, a 3D image can be obtained, in which the amplitude of the impulse received by the antenna is commuted into a colored scale. The use of 3D imaging becomes mainly important when used as a means of communicating complex information to the wider archaeological community. The 3D visualization it is important to understand and properly interpret the more traditional 2D forms of GPR data representation.

The 3D visualization was carried out with Mala, Reflexw and GPR-Slice. The 3D visualization results indicate the existence mean anomaly at round 20 ns (1 m depth) (figure 4).

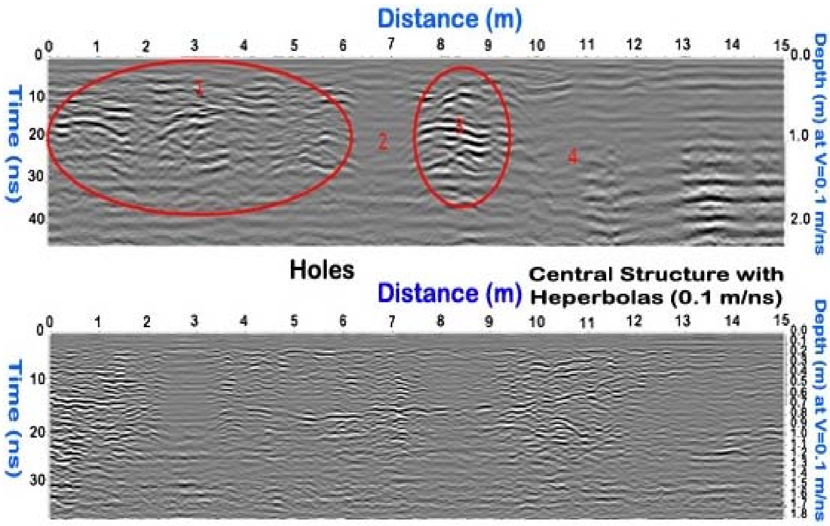

Figure 8: Processed Radargrams (Area 8) (B-Scan) achievement with 500 MHz antenna from line 07 (A) and with 800 MHz antenna from line 28 (B)

Area 7

The GPR undertaken at Turaniana in Almeria has identified a number of area anomalies that may be of an archaeological origin. Examples of these features can be seen in figure 5.

Figure 5 shows a radargrams obtained with the 500 MHz and 800 MHz antenna. The following processing sequences were filtered before interpretation (Table 2).

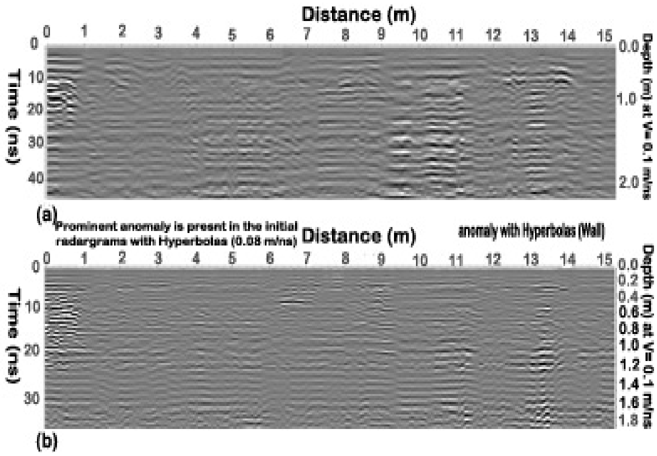

Figure 5: Processed Radargrams (Area 7) (B-Scan) achievement with 500 MHz antenna from line 3 (a) and with 800 MHz antenna from line 3 (b**)**

Figure (5a-5b) shows the interpretation of the processed radargrams which present some structural characteristics that can be easily identified as the walls or others archaeological remains. Observing the radargrams in Figure 5(a-b) it is possible to identify the hyperbolic reflection. This reflection situated between 0 and 1.25 meters at round 8-20 ns (0.5 m- 1.25 m depth) could be related to the presence of a anomalies that are may be related to buried structural.

Time slices were obtained at various times by calculating 2D amplitude maps of the radar signals, using specified time window in all parallel and perpendicular radar profiles. The color scale is normalized to the maximum reflection obtained in the slice.

In area 7, multiple anomalies are found as can be seen in the C-scans approximately between 5- 20 ns roughly corresponding to a depth of 0.3- 1.1 m shown in figure 6. It is easy to recognize shapes and lateral extensions of the various structures and walls between 0- 8 m.

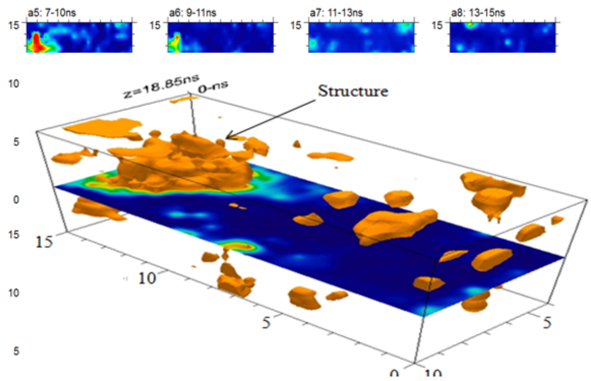

Figure 10: GPR-slice iso-surface renders and times-slices obtained in the time windows 5-40ns with 800 MHz antenna

The mean anomalies showed in the time slice can perhaps be ascribed to the boundary of the archaeological Roman remains.

3D GPR data acquisition, processing, and interpretation seems to be inevitable to thoroughly interpret and understand complex subsurface structures typically found at archaeological sites. The extraction of a 3D volume which represents the target was possible by using the isosurface rendering technique. This technique displays surfaces of equal amplitude in the 3D volume.

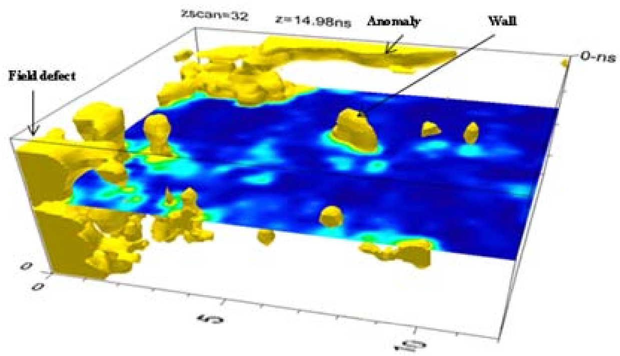

Figure 7: GPR-slice iso-surface renders and times-slices obtained in the time windows 0-30ns with 500 MHz antenna

Figure 7 showed the initial anomalies at around 5- 22ns. These anomalies indicate the presence of the walls or house foundations.

Area 8

Figure 8 shows a GPR profile of 500 MHz and 800 MHz antenna. Figure 8a clearly shows numerous strong radar reflections from 0 at 6m distance at around 5 -30 ns (0.2 -1.6 m depth) (denote 1). The modern utility ditch creates a strong reflection from 6-7.6 m and 9.8 -11 m distance and extending slightly more than two meter below ground (red circle denote 2 and 4). Some deep structures are observable, especially on the right hand side from 7.5 - 9.5 m distance (denote 3). When interpreting the sections, one looks for discontinuities in the events or apparent amplitude variations. Buried objects are often localized by the presence of point diffractions, which result in flattened hyperbolic patterns of energy.

Figure 8b obtained by the 800 MHz antenna shows strong reflectors at 0.2- 1.5 m depth (5- 25 ns time slice) and great hyperbola with velocity 0.1 m/ns. This hypothesis will be studied in Appendix.

These main anomalies can identify the size, shape, depth, and location of buried archeological remains.

The 2D processing of the data and its visualization as time slices improved the datasets and the interpretation of the anomalies.

Figure 9 shows the main anomalies at around 22- 37 ns (1- 1.6 m depth) related to the foundation. Further anomalies might represent the remains of the original of the walls of a stone burial.

GPR has the ability to create pseudo 3D maps and images of buried archaeological and other associated cultural and natural features. Usually the pseudo 3D time slices give information on the planar distribution of the buried targets at different depths, whereas the 3D maps show the full geometry of the targets.

Figure 10 illustrates the 3D imaging result for a main anomaly associated with structure at around 22 ns.

Area 9

Data processing and modeling aim to search for and visualize anomalous structures and to present results in maps.

Figure 11 shows two radargrams achievement with 500 MHz and 800 MHz antennas of the survey carried out in area 9.

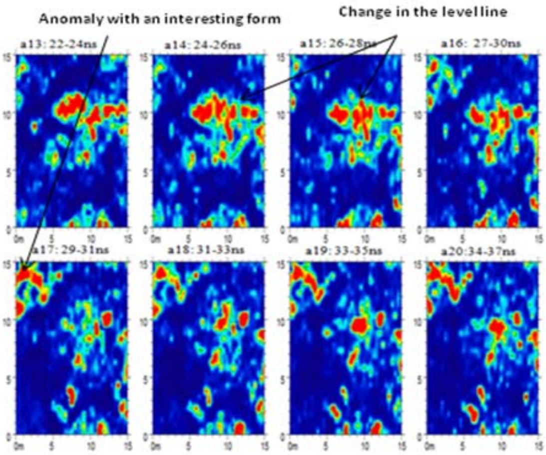

Figure 9: Time-Slice (C-Scan) of area 8 at 22ns-37 ns with 500 MHz antenna

Distinctive point source reflections of buried structures (structures 1 and 2) were visible in some profile between 3.5 m - 5.5 m and 14 m - 15.5 m distance at around 3 ns - 20 ns (Fig.11 (a-b)). It is probable that these point source reflections are the record of reflections that occurred from the walls. These hyperbolic reflections were used to map all visible buried structures. This hypothesis will be studied in Appendix.

GPR provides us with depth information of the structures which can help the archaeologists in planning.

In this area, the mean anomalies can be clearly seen in the time slice. In Fig.12, in the right-hand part of this area, precisely from 5 to 10 m of the abscissa (3 ns – 20 ns), some structures (same as those seen in radargrams showed in figure 11) can be located starting from approximate depth of 0.2 m – 1 m. These structures are possibly due to presence of portion of walls or houses foundations.

The particular geometry suggests that 3D processing and visualization would be better suited to properly take into account 3D effects.

The 3D imaging results illustrate two structures at distance 3.5 m- 5.5 m and 14 m- 15.5 m (3 ns – 20 ns) and surface anomalies at around 2ns- 7 ns (Fig. 13). These structures can be interpreted of the portion of the walls or house foundation or Roman archaeological remains.

The detail in the 3D data has proven useful for detailed detection of small objects in and around the wreck.

Conclusion

The use of Geo-sensing methods employing equipment such as the Ground Penetrating Radar serves as a significant aid in detecting hidden objects over large areas in a relatively quicker and accurate way while ensuring that it remains noninvasive. The work described in this essay focused on the archaeological site of Roquetas de Mar and the GPR survey presented several locations that offer the most promising prospect of further investigation and excavation to aid archaeologists. Certain targets within the analyzed zones created unique GPR reflections which provide further insight into possible sub surface anomalies. The use of 3D visualization tools allowed for a detailed insight into very small zones within the large areas mapped and offers a significantly improved head start to investigators looking for anomalies within the area.

Appendix

Simulation of Reflexw using Finite Difference Time Domain (FDTD)

The Finite Difference Time Domain (FDTD) method has proven to be one of the most popular techniques reported in literature. Reasons for this are that the FDTD approach is conceptually simple in contrast to other methods, is accurate for arbitrarily complex models, and is capable of accommodating realistic antenna designs and important features such as dispersion in electrical properties [11][12].

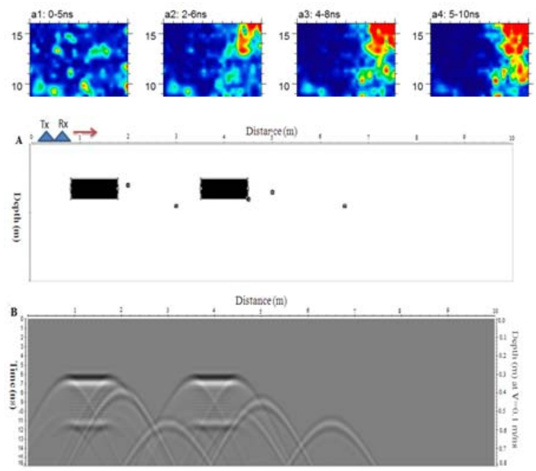

Figure 14: FDTD models showing the effect produced dry sand and wall. A: models; B: synthetic radargrams.

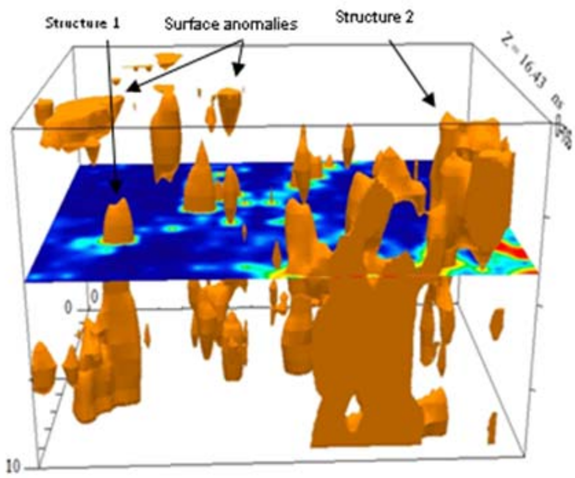

Figure 13: GPR-slice iso-surface renders and times-slices obtained in the time windows 0-22 ns with 500 MHz antenna

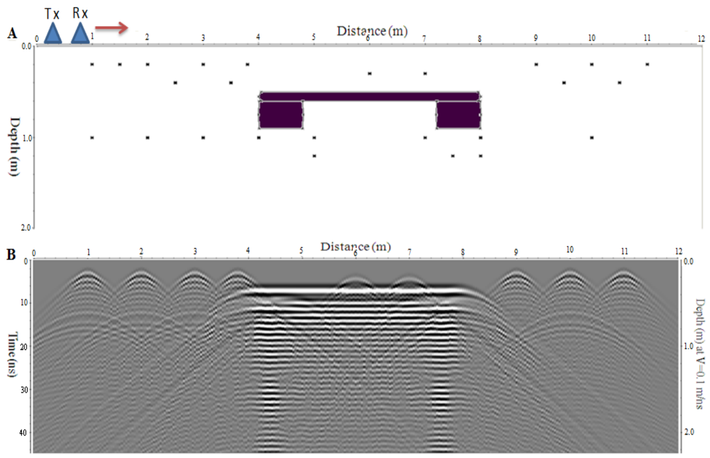

Figure 15: FDTD models showing the effect produced dry sand and other construction. A: models; B: synthetic radargrams

Most models were created using the modeling module supplied as part of Reflexw [10]. In addition to its modeling module, this commercial software offers a number of 2D modules designed to process and analyze seismic and GPR data. It's modeling module, arbitrary shapes can easily be defined and modified.

In the area 8, some circular forms were noticed (Fig. 9). These circular forms were formed by gaps in horizontal reflections. Here it will be investigated whether these forms could be caused by holes or broken of walls or foundations. The scenario suggested verifying this is shown in figure 14a.

Figure 14a show the first model consisting of a dry sand (white) ground where two part of wall is buried at 0.5 m depth (black) and some clutter is added as small stones (radius= 25mm) (black) of random location. Both antennas, transmitter (Tx) and receiver (Rx), move together parallel to the ground with a spatial step of electrical properties of the material used are dry sand (white) ($\varepsilon_r = 3, \mu = 1, \sigma = 0.0001\ S/m$) and wall (black) ($\varepsilon_r = 5.5, \mu = 1, \sigma = 0.042\ S/m$). The signals refracted by this model were simulated and analyzed using the software Reflexw, for central frequency of f_m = 3*500 MHz. This frequency corresponds to wave length directed in the simulated medium:

$$\lambda = \frac{c}{f_m\sqrt{\varepsilon_r}} = \frac{3.10^8}{3.500.10^6.\sqrt{3}} = 0.115 \text{ m}$$

An example of the geometrical model used for modeling of the radar signal refracted from wall. Each signal emission and reflection is recorded during a time-period of 27 ns with a spatial increment $\Delta x = \Delta y = \Delta l = \frac{\lambda}{10} = 0.0115$ m. The total simulated length is 10 m x 2.0 m and the ricker source excitation can be used to simulate the GPR antenna.

The synthetic radargrams (Fig.14b) reveal the capability of the 500 MHz antenna to detect the target. This radargrams shows the hyperbole resulting from wave reflections of the targets. It can be also seen two horizontal reflections at 6 ns terminated by edge diffractions corresponds to the wall.

The second model (Fig.15a) was designed to represent another construction technique often found in archeological sites. The compacted earth floor model was modified to represent wall ($\varepsilon_r = 5.5, \mu = 1, \sigma = 0.042\ S/m$) (black) and included wall stubs at the edges of the floor. The signals refracted by this model were simulated for same frequency used previously. The total simulated length is 12 m x 2 m.

Figure 15b illustrates the radargrams and exhibits some of the model seen in figure 11a. The multi-layer floor creates multiple parallel horizontal reflections. Each stone presents within the walls produced diffractions at its edges indicating the complex constructions of the walls.

Acknowledgment

The work described in this paper and the research leading to these results has received funding from the European Community’s Seventh Framework Programme FP7/2007-2013, under grant agreement no 205294 (HIRF–SE project), and from the Spanish National Projects TEC2010-20841-C04-04, CSD2008-00068, and the Junta de Andaluc´ ıa Project P09-TIC-5327.

References

[1] A. Bhuiyan and B. Nath, “Anti-personnel mine detection and classification using gpr image,” Proceedings of the Inernational conference on Pattern Recognition, vol. 2, p. 10821085, 2006.

[2] G. Grandjean and J. C. Gourry, “Gpr data processing for 3d fracture mapping in a marble quarry (thassos, greece),” Journal of Applied Geophysics, vol. 36, no. 1, pp. 19–30, 1996.

[3] R. Jack and P. Jackson, “Imaging attributes of railway track formation and ballast using ground probing radar,” NDT & E International, vol. 32, no. 8, pp. 457–462, 1999.

[4] F. A. Shaaban, A. M. Abbas, M. A. Atya, and M. A. Hafez, “Ground-penetrating radar exploration for ancient monuments at the valley of mummies -kilo 6, bahariya oasis, egypt,” Journal of Applied Geophysics,vol. 68, no. 2, pp. 194 – 202, 2009.

[5] M. Edwards, W.; Okita and D. Goodman, “Investigation of a subterranean tomb in miyazaki, japan,” Archaeological Prospection, vol. 7, no. 4, p. 215224, 2000.

[6] Goodman, D, J. Steinberg, B. Damiata, Y. Nishimura, K. Schneider, H. Hiromichi, N. Higashi. 2006. GPR Overlay Analysis for Archaeological Prospection. Proceedings of the 11th International Conference on Ground Penetrating Radar 2006, Columbus, Ohio, USA.

[7] Grasmueck, M. and D.A. Viggiano. 2007. Integration of Ground-Penetrating Radar and Laser Positioning Sensors for Real-Time 3-D Data Fusion. IEEE Transactions on Geoscience and Remote Sensing, vol 45, N. 1, January 2007.

[8] Groenenboom, J., J. van der Kruk and J.H. Zeeman. 2001. 3D GPR data acquisition and the influence of positioning errors on image quality. 63rd EAGE Conference and Technical Exhibition, Amsterdam, 11-15 June 2201, 4 pp.

[9] Leckebusch, J. 2003. Ground-Penetrating Radar: A Modern Three-dimensional Prospection Method. Archaeological Prospection, 10, 213-240.

[10] K.J. Sandmeier, Reflexw Version 4.5. Licence number 597 Licenced to centro tecnologico del Marmol y la Piedra Spain

[11] Gurel, Levent and Ugur Oguz. 2001. Simulations of Ground Penetrating Radar over lossy and Heterogenous Grounds. IEEE Transaction Geosciences and Remote Sensing 39: 1190-1197.

[12] Irving, James D., and Rosemary J. Knight. 2006 Numerical Modeling of Ground Penetrating Radar in 2-D using Matlab. Computers & Geosciences 32: 1247-1258.

[13] A. Giannopoulos, Modelling ground penetrating radar by GprMax, Construction and Building Materials 19 (10) (2005) 755–762.